Central European Journal of Energetic Materials
ISSN 1733-7178; e-ISSN 2353-1843

Cent. Eur. J. Energ. Mater. 2019, *16*(3): 412-432; DOI 10.22211/cejem/112306
Article is available in PDF-format, in colour, at:
http://www.wydawnictwa.ipo.waw.pl/cejem/Vol-16-Number3-2019/CEJEM_00978.pdf

Research paper

Prediction of the Crystalline Densities of Aliphatic Nitrates by Quantum Chemistry Methods

Guixiang Wang,* Yimin Xu, Chuang Xue, Zhiyuan Ding, Yan Liu, Hui Liu, Xuedong Gong**

Computation Institute for Molecules and Materials, Department of Chemistry, Nanjing University of Science and Technology, Nanjing 210094, China
E-mails: * wanggx1028@163.com; ** gongxd325@mail.njust.edu.cn

Abstract: Crystal density is a basic and important parameter for predicting the detonation performance of explosives, and nitrate esters are a type of compound widely used in the military context. In this study, thirty-one aliphatic nitrates were investigated using the density functional theory method (B3LYP) in combination with six basis sets (3-21G, 6-31G, 6-31G*, 6-31G**, 6-311G* and 6-31+G**) and the semiempirical molecular orbital method (PM3). Based on the geometric optimizations at various theoretical levels, the molecular volumes and densities were calculated. Compared with the available experimental data, the densities calculated by various methods are all overestimated, and the errors of the PM3 and B3LYP/3-21G methods are larger than those of other methods. Considering the results and the computer resources required by the calculations, the B3LYP/6-31G* method is recommended for predicting the crystalline densities of organic nitrates using a fitting equation. The results obtained with this method are slightly better than those reported by Keshavarz and Rice. In addition, the effects of various groups (such as $–ONO_2$, –OH, –Cl, –O–, and $–CH_2–$) on the densities are also discussed, which is helpful for the design of new molecules in terms of practical requirements.

Keywords: aliphatic nitrates, density, quantum chemistry, correlation

Nomenclature:

D difference between the predicted and experimental densities [g·cm^{-3}]
V molecular volume [cm^3·mol^{-1}]
ρ crystalline density [g·cm^{-3}]

1 Introduction

Currently, the study of novel high energy density materials (HEDMs) is one of the most active regions of research and seems to be never ending because of the superior explosive performances of HEDMs compared to the currently used materials [1-3]. Density is a primary physical parameter, closely related to the explosive performances such as detonation velocity and pressure, explosion heat, and specific volume. Since detonation velocity and detonation pressure increase proportionally with the density and the square of the density, respectively [4, 5], improving the density is the main approach to discovering new HEDMs at present. It is thus very important to obtain the density of proposed new compounds.

Among the methods previously used to predict the crystalline density (ρ_{exp}) of explosives, the simplest, earliest and most widely used one is the group additivity method of the molar refraction [5] and the molar volume [6, 7], where the molar volume is obtained by summing up the volumes of atoms or functional groups. These methods can rapidly predict the volume and density. However, they have limitations in accounting for the molecular conformation, isomerization, and crystal packing efficiency.

Researchers [8-13] have also been attempting to use the potential function and crystal chemistry methods, based on the dense packing theory, to predict crystalline densities more accurately. These approaches can effectively account for the influence of the molecular spatial arrangement, but they require extensive computational work and take more computer time and higher costs, which makes it difficult for wide application.

Keshavarz *et al.* [14-21] developed some new correlations to predict explosive parameters simply from the number of carbon, hydrogen and nitrogen atoms and other structural parameters for nitroaromatic and nitroaliphatic compounds, acyclic and cyclic nitramines, nitrate esters, polynitro arene and polynitro heteroarene explosives, *etc.*

In order to better account for the intermolecular interactions in C,H,O,N crystals, Politzer *et al.* [22, 23] developed a procedure with an electrostatic interaction correction to predict the crystalline densities for both neutral and ionic molecular crystals at the B3PW91/6-31G** level of density functional theory (DFT),

and reported two equations (*viz.* Equations 1 and 2) to predict the crystalline densities of neutral molecules:

$$\rho=\alpha_1 \frac{M}{V_m}+\beta_1(\nu\sigma_{tot}^{\ 2})+\gamma_1 \quad (1)$$

$$\rho=\alpha_2 \frac{M}{V_m}+\beta_2(\Pi)+\gamma_2 \quad (2)$$

where M is the molecular weight, V_m is the volume inside the 0.001 a.u. isosurface of electron density surrounding the molecule, calculated at the B3PW91/6-31G** level, σ_{tot}^2 and $\prod$ are the total and the average deviation variances of the electrostatic potential on the 0.001 a.u. surface, v is an electrostatic balance parameter, α_1, β_1, γ_1, and α_2, β_2, γ_2 are coefficients which are available from Ref. [22].

Later, Rice *et al.* [24] used the procedure of Politzer *et al.* [22, 23] to predict the crystalline densities of neutral and ionic compounds at the B3LYP/6-31G** level. In recent years, our group has proposed a new efficient method to predict the density (ρ_{cal}) based on the quantum chemistry calculation of molecular volume. This method has been widely used in calculating the detonation properties of the organic cage compounds and heterocyclic nitramines, and plays an important role in "molecular design" of high energy density compounds (HEDCs) and materials (HEDMs) [25-31].

Qiu *et al.* [32] performed a quantum chemistry study on 45 energetic nitramines and compared the calculated density ρ_{cal} with the experimental value ρ_{exp}. They found that, on the whole, ρ_{cal} calculated at the B3LYP/6-31G** level of the density functional theory (DFT) accords with ρ_{exp}, whereas using the B3LYP functional with a larger basis set underestimates $\rho_{cal.}$, and the densities are all overestimated by the semiempirical molecular orbital methods.

Is this conclusion applicable for other kinds of explosives? For various kinds of explosives, do the densities calculated by different methods have such regularities? In view of these problems, we have further researched [33] thirty nitro aromatic compounds using the B3LYP functional of DFT with six basis sets and the semiempirical PM3 method. It was found that ρ_{cal} estimated by the PM3 and B3LYP/3-21G methods are all larger than ρ_{exp}, and those obtained with the other five basis sets are better and quite accurate. Considering that a larger basis set demands more computer resources, B3LYP/6-31G or B3LYP/6-31G* is recommended to rapidly and reliably predict the crystalline densities of polynitroarenes.

To further test the reliability and applicability of our conclusions, another important kind of compound, namely aliphatic nitrates (see Figure 1 for the structural diagrams) is studied in detail in this paper. Aliphatic nitrates, such as methyl nitrate (MN), ethylene glycol dinitrate (EGDN), nitroglycerine (NG), butanetriol trinitrate (BTTN), pentaerythritol tetranitrate (PETN), *etc.*, as a type of multifunctional material, have been receiving considerable attention and many investigation [34-37]. Various theoretical methods are used. The results from different methods are compared and the effects of the methods on the densities are discussed. The conclusions may be useful for the molecular design and further studies of novel HEDMs.

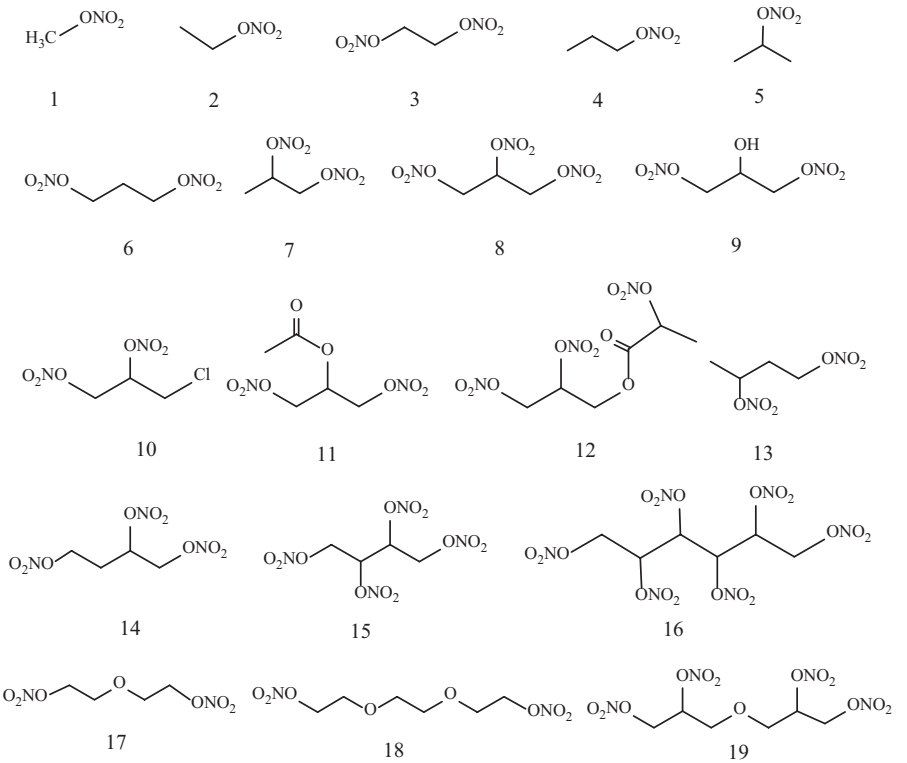

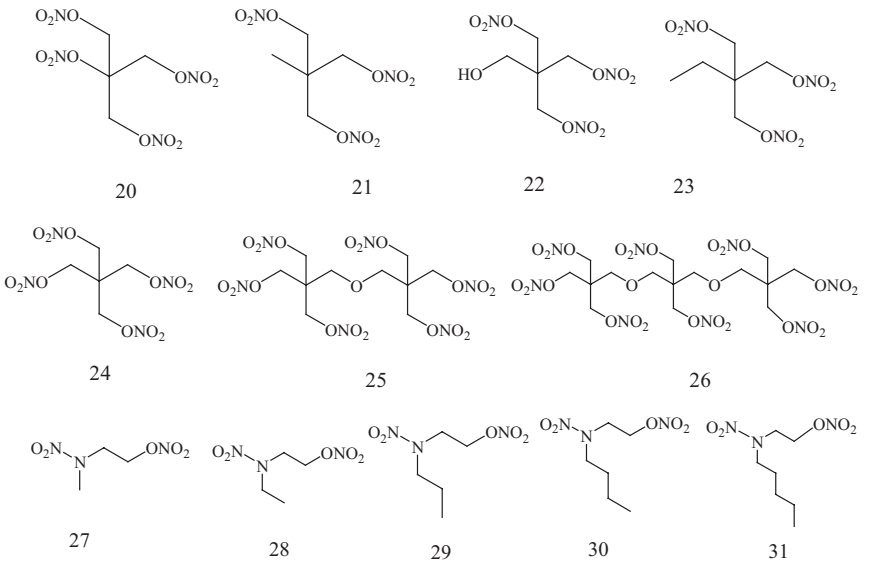

Figure 1. Illustration of the molecular structures of the aliphatic nitrates

2 Computational Method

Thirty-one aliphatic nitrates were fully optimized without any symmetry restrictions with the semiempirical PM3 [38] method and the B3LYP functional [39, 40] of DFT with the 3-21G, 6-31G, 6-31G*, 6-31G**, 6-311G* and 6-31+G** basis sets [41-45]. To characterize the nature of the stationary points, harmonic vibrational analyses were performed on each optimized structure, which demonstrated that all of the optimized structures are local energy minima on the potential energy surface (PES) without presentation of the imaginary frequency.

The density of each compound was obtained from the molecular weight (M) divided by the volume (V). The volume is defined as the space inside the 0.001 e/bohr^3 electron density surface and obtained from the statistical average of 100 volume calculations using the Monte-Carlo method with the Gaussian03 program package [46].

3 Results and Discussion

3.1 Effect of the method on density

Tables 1 and 2 lists the molecular volume (V) and density (ρ_{cal}), respectively, predicted with the different methods and basis sets. For comparison, the corresponding experimental density (ρ_{exp}), error, and root mean square error (Rms) are also listed in Table 2.

The data in Table 1 show that the volumes obtained from PM3 and B3LYP/3-21G are smaller than those from other methods. On the whole, the larger the basis set (from 6-31G to 6-31+G**), the larger the volume, *i.e.* a larger basis set makes the occupied space of the electrons larger. In addition, we also found that the volumes increased with an increasing number of $–ONO_2$, –OH, –Cl, $–CH_2–$, $–N–NO_2$, and $–CH_3$ groups, obviously showing group additivity. For Me-NENA (27), Et-NENA (28), Pr-NENA (29), Bu-NENA (30), and Pt-NENA (31), the volumes obtained from various DFT methods increase with an increasing number of methylene ($–CH_2–$) groups, and there are good linear correlations. For example, for the B3LYP/6-31G* method, the correlation equation (Equation 3) is:

$$V = 102.55 + 13.78n \quad (3)$$

and the corresponding correlation coefficient is 0.9986. Besides, the differences in volume between the isomers, such as between *n*-PN (4) and *iso*-PN (5), and between 1,3-PGDN (6) and 1,2-PGDN (7) (see Table 1), is small, indicating that the space orientations of the substituent groups have little influence on the volume. To show the variation of V with different methods and basis sets more clearly, Figure 2 is presented to show the correlations between the structures and Vs obtained with the different methods.

Table 1. Molecular volumes obtained from different methods

No.	Compound (Code)	V [cm^3·mol^{-1}]						
		PM3	3-21G	6-31G	6-31G*	6-31G**	6-311G*	6-31+G**
1	Methyl nitrate (MN)	43.69	44.74	50.24	49.54	50.16	51.32	51.06
2	Ethyl nitrate (EN)	57.95	59.04	63.57	63.49	62.72	66.27	65.35
3	Ethylene glycol dinitrate (EGDN)	77.27	82.20	87.00	86.83	88.39	87.46	90.64
4	*n*-Propyl nitrate (*n*-PN)	71.93	73.52	78.27	78.18	78.10	77.30	78.66
5	*iso*-Propyl nitrate (*iso*-PN)	71.79	74.78	79.02	76.96	76.77	78.76	78.06
6	1,3-Propylene glycol dinitrate (1,3-PGDN)	91.96	94.01	105.46	101.15	102.09	102.09	102.88
7	1,2-Propylene glycol dinitrate (1,2-PGDN)	93.73	96.49	102.64	102.83	102.04	101.29	104.99
8	Nitroglycerine (NG)	106.66	114.28	125.84	126.99	126.53	129.54	127.08
9	Glycerine-1,3-dinitrate(GDN)	93.94	98.23	106.77	105.74	106.34	109.02	108.69
10	Glycerine chlorohydrin dinitrate (GCDN)	99.59	105.64	115.42	115.42	116.30	115.92	115.39
11	Glycerol acetate dinitrate (GADN)	121.53	127.05	137.73	134.81	134.67	139.36	137.94
12	Glycerol monolactate trinitrate	154.54	163.53	175.90	172.34	172.51	173.14	180.69
13	1,3-Butylene glycol dinitrate (1,2-BGDN)	105.69	106.13	117.08	114.93	113.55	115.65	114.79
14	1,2,4-Butanetriol trinitrate (1,2,4-BTTN)	124.53	127.02	140.62	139.19	138.69	140.83	140.61
15	Erythritol tetranitrate (ETetN)	140.82	149.58	165.52	160.49	160.88	166.12	165.37
16	Mannitol hexanitrate (MHN)	208.29	219.44	238.52	237.71	236.26	236.37	245.72
17	Diethylene glycol dinitrate (DEGDN)	113.16	112.17	125.66	122.41	124.03	122.00	126.05
18	Triethylene glycol dinitrate (TEGDN)	147.19	148.76	161.36	153.88	158.25	157.50	160.84
19	Diglycerin tetranitrate (DGTN)	176.67	178.98	200.04	197.83	196.46	197.87	201.72
20	Trimethylolnitratomethane trinitrate (TMNMTN)	138.49	141.93	157.54	151.51	156.85	156.35	161.12
21	Trimethylolethane trinitrate (TMETN)	134.27	138.38	153.16	151.76	152.00	150.89	154.62
22	Pentaerthritol trinitrate (PETriN)	141.21	143.78	158.40	153.50	157.96	157.16	158.81
23	Trimethylolpropane trinitrate (TMPTN)	152.01	150.71	169.39	164.80	164.47	168.76	172.50
24	Pentaerythritol tetranitrate (PETN)	153.20	160.58	179.22	172.33	176.56	175.01	181.28

25	Dipentaerthritol hexanitrate (DPEHN)	266.79	276.84	299.63	294.25	297.37	304.41	305.34
26	Tripentaerthritol octanitrate (TPEON)	383.86	379.37	416.15	417.39	424.86	422.68	432.37
27	*N*-Methyl-2-nitrato-ethyl nitramine (Me-NENA)	97.22	94.99	102.77	103.73	103.78	105.00	104.84
28	*N*-Ethyl-2-nitrato-ethyl nitramine (Et-NENA)	110.38	111.71	116.83	114.60	120.02	117.17	121.91
29	*N*-Propyl-2-nitrato-ethyl nitramine (Pr-NENA)	123.69	125.15	132.53	129.88	132.06	135.61	133.53
30	*N*-Butyl-2-nitrato-ethyl nitramine (Bu-NENA)	138.88	136.43	147.21	144.82	145.62	148.25	148.53
31	*N*-Pentyl-2-nitrato-ethyl nitramine (Pt-NENA)	150.46	150.79	159.44	157.53	157.76	161.35	161.21

Table 2. Densities (ρ_{exp} is taken from Refs. [47-51]) obtained from different methods

No.	Compound (Code)	ρ_{exp} [g·cm^{-3}]	ρ_{cal} and – in brackets – deviations of the calculated results from the experimental values [$g \cdot cm^{-3}$]						
			PM3	3-21G	6-31G	6-31G*	6-31G**	6-311G*	6-31+G**
1	Methyl nitrate (MN)	**1.22**	**1.76**	**1.72**	**1.53**	**1.56**	**1.54**	**1.50**	**1.51**
			(0.54)	(0.50)	(0.31)	(0.34)	(0.32)	(0.28)	(0.29)
2	Ethyl nitrate (EN)	**1.10**	**1.57**	**1.54**	**1.43**	**1.43**	**1.45**	**1.37**	**1.39**
			(0.47)	(0.44)	(0.33)	(0.33)	(0.35)	(0.27)	(0.29)
3	Ethylene glycol dinitrate (EGDN)	**1.48**	**1.97**	**1.85**	**1.75**	**1.75**	**1.72**	**1.74**	**1.68**
			(0.49)	(0.37)	(0.27)	(0.27)	(0.24)	(0.26)	(0.20)
4	*n*-Propyl nitrate (*n*-PN)	**1.06**	**1.46**	**1.43**	**1.34**	**1.34**	**1.35**	**1.36**	**1.34**
			(0.40)	(0.37)	(0.28)	(0.28)	(0.29)	(0.30)	(0.28)
5	*iso*-Propyl nitrate (*iso*-PN)	**1.04**	**1.46**	**1.41**	**1.33**	**1.37**	**1.37**	**1.33**	**1.35**
			(0.42)	(0.37)	(0.29)	(0.33)	(0.33)	(0.29)	(0.31)
6	1,3-Propylene glycol dinitrate (1,3-PGDN)	**1.39**	**1.81**	**1.77**	**1.57**	**1.64**	**1.63**	**1.63**	**1.61**
			(0.42)	(0.38)	(0.18)	(0.25)	(0.24)	(0.24)	(0.22)
7	1,2-Propylene glycol dinitrate (1,2-PGDN)	**1.37**	**1.77**	**1.72**	**1.62**	**1.62**	**1.63**	**1.64**	**1.58**
			(0.40)	(0.35)	(0.25)	(0.25)	(0.26)	(0.27)	(0.21)

8	Nitroglycerine (NG)	**1.60**	**2.13**	**1.99**	**1.80**	**1.79**	**1.79**	**1.75**	**1.79**
			(0.53)	(0.39)	(0.20)	(0.19)	(0.19)	(0.15)	(0.19)
9	Glycerine-1,3-dinitrate(GDN)	**1.52**	**1.94**	**1.85**	**1.71**	**1.72**	**1.71**	**1.67**	**1.68**
			(0.42)	(0.33)	(0.19)	(0.20)	(0.19)	(0.15)	(0.16)
10	Glycerine chlorohydrin dinitrate (GCDN)	**1.53**	**2.01**	**1.90**	**1.74**	**1.74**	**1.72**	**1.73**	**1.74**
			(0.48)	(0.37)	(0.21)	(0.21)	(0.19)	(0.20)	(0.21)
11	Glycerol acetate dinitrate (GADN)	**1.41**	**1.84**	**1.76**	**1.63**	**1.66**	**1.66**	**1.61**	**1.62**
			(0.43)	(0.35)	(0.22)	(0.25)	(0.25)	(0.20)	(0.21)
12	Glycerol monolactate trinitrate	**1.47**	**1.94**	**1.83**	**1.70**	**1.74**	**1.73**	**1.73**	**1.66**
			(0.47)	(0.36)	(0.23)	(0.27)	(0.26)	(0.26)	(0.19)
13	1,3-Butylene glycol dinitrate (1,2-BGDN)	**1.32**	**1.70**	**1.70**	**1.54**	**1.57**	**1.59**	**1.56**	**1.57**
			(0.38)	(0.38)	(0.22)	(0.25)	(0.27)	(0.24)	(0.25)
14	1,2,4-Butanetriol trinitrate (1,2,4-BTTN)	**1.52**	**1.94**	**1.90**	**1.71**	**1.73**	**1.74**	**1.71**	**1.71**
			(0.42)	(0.38)	(0.19)	(0.21)	(0.22)	(0.19)	(0.19)
15	Erythritol tetranitrate (ETetN)	**1.60**	**2.15**	**2.02**	**1.83**	**1.88**	**1.88**	**1.82**	**1.83**
			(0.55)	(0.42)	(0.23)	(0.28)	(0.28)	(0.22)	(0.23)
16	Mannitol hexanitrate (MHN)	**1.73**	**2.17**	**2.06**	**1.90**	**1.90**	**1.91**	**1.91**	**1.84**
			(0.44)	(0.33)	(0.17)	(0.17)	(0.18)	(0.18)	(0.11)
17	Diethylene glycol dinitrate (DEGDN)	**1.38**	**1.73**	**1.75**	**1.56**	**1.60**	**1.58**	**1.61**	**1.56**
			(0.35)	(0.37)	(0.18)	(0.22)	(0.20)	(0.23)	(0.18)
18	Triethylene glycol dinitrate (TEGDN)	**1.34**	**1.63**	**1.61**	**1.49**	**1.56**	**1.52**	**1.52**	**1.49**
			(0.29)	(0.27)	(0.15)	(0.22)	(0.18)	(0.18)	(0.15)
19	Diglycerin tetranitrate (DGTN)	**1.52**	**1.96**	**1.93**	**1.73**	**1.75**	**1.76**	**1.75**	**1.72**
			(0.44)	(0.41)	(0.21)	(0.23)	(0.24)	(0.23)	(0.20)
20	Trimethylolnitratomethane trinitrate (TMNMTN)	**1.64**	**2.07**	**2.02**	**1.82**	**1.89**	**1.82**	**1.83**	**1.78**
			(0.43)	(0.38)	(0.18)	(0.25)	(0.18)	(0.19)	(0.14)

21	Trimethylolethane trinitrate (TMETN)	**1.47**	**1.90**	**1.84**	**1.67**	**1.68**	**1.68**	**1.69**	**1.65**
			(0.43)	(0.37)	(0.20)	(0.21)	(0.21)	(0.22)	(0.18)
22	Pentaerthritol trinitrate (PETriN)	**1.54**	**1.92**	**1.89**	**1.71**	**1.77**	**1.72**	**1.73**	**1.71**
			(0.38)	(0.35)	(0.17)	(0.23)	(0.18)	(0.19)	(0.17)
23	Trimethylolpropane trinitrate (TMPTN)	**1.50**	**1.77**	**1.79**	**1.59**	**1.63**	**1.64**	**1.59**	**1.56**
			(0.27)	(0.29)	(0.09)	(0.13)	(0.14)	(0.09)	(0.06)
24	Pentaerythritol tetranitrate (PETN)	**1.77**	**2.06**	**1.97**	**1.76**	**1.83**	**1.79**	**1.81**	**1.74**
			(0.29)	(0.20)	(–0.01)	(0.06)	(0.02)	(0.04)	(–0.03)
25	Dipentaerthritol hexanitrate (DPEHN)	**1.63**	**1.97**	**1.89**	**1.75**	**1.78**	**1.76**	**1.72**	**1.72**
			(0.34)	(0.26)	(0.12)	(0.15)	(0.13)	(0.09)	(0.09)
26	Tripentaerthritol octanitrate (TPEON)	**1.58**	**1.91**	**1.93**	**1.76**	**1.75**	**1.72**	**1.73**	**1.69**
			(0.33)	(0.35)	(0.18)	(0.17)	(0.14)	(0.15)	(0.11)
27	*N*-Methyl-2-nitrato-ethyl nitramine (Me-NENA)	**1.53**	**1.70**	**1.74**	**1.61**	**1.59**	**1.59**	**1.57**	**1.57**
			(0.17)	(0.21)	(0.08)	(0.06)	(0.06)	(0.04)	(0.04)
28	*N*-Ethyl-2-nitrato-ethyl nitramine (Et-NENA)	**1.32**	**1.62**	**1.60**	**1.53**	**1.56**	**1.49**	**1.53**	**1.47**
			(0.30)	(0.28)	(0.21)	(0.24)	(0.17)	(0.21)	(0.15)
29	*N*-Propyl-2-nitrato-ethyl nitramine (Pr-NENA)	**1.26**	**1.56**	**1.54**	**1.46**	**1.49**	**1.46**	**1.42**	**1.45**
			(0.30)	(0.28)	(0.20)	(0.23)	(0.20)	(0.16)	(0.19)
30	*N*-Butyl-2-nitrato-ethyl nitramine (Bu-NENA)	**1.21**	**1.49**	**1.52**	**1.41**	**1.43**	**1.42**	**1.40**	**1.39**
			(0.28)	(0.31)	(0.20)	(0.22)	(0.21)	(0.19)	(0.18)
31	*N*-Pentyl-2-nitrato-ethyl nitramine (Pt-NENA)	**1.18**	**1.47**	**1.47**	**1.39**	**1.40**	**1.40**	**1.37**	**1.37**
			(0.29)	(0.29)	(0.21)	(0.22)	(0.22)	(0.19)	(0.19)
Average absolute error, *Daa*			(0.39)	(0.35)	(0.20)	(0.22)	(0.21)	(0.20)	(0.18)
Root mean square error, *Drms*			(0.40)	(0.35)	(0.21)	(0.23)	(0.22)	(0.21)	(0.19)

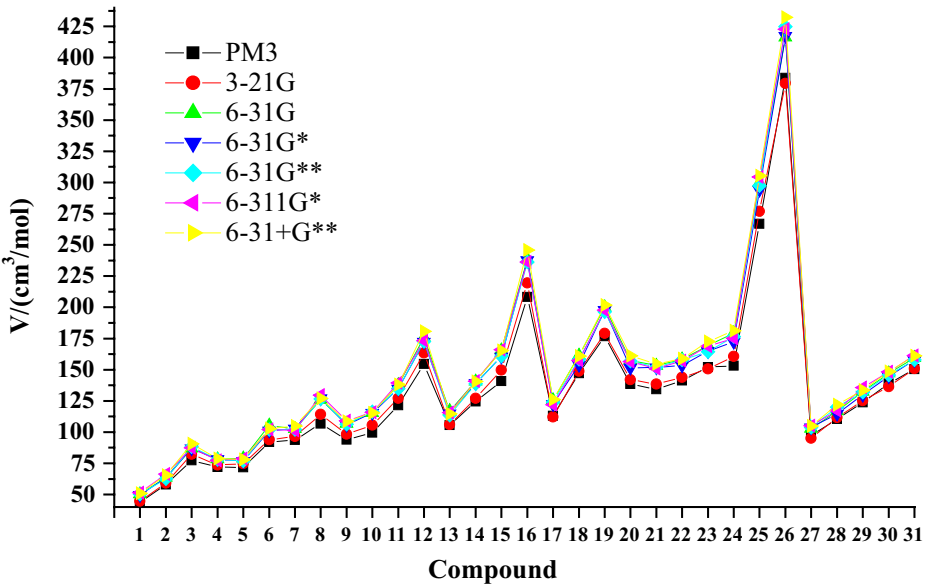

Figure 2. Correlations between structures and volumes calculated by various methods

Unlike the nitramines [32] and nitroaromatic compounds [33], for all aliphatic nitrates, the densities calculated by various methods (ρ_{cal}) are all overestimated, *i.e.* the theoretical densities are larger than the experimental data, with the average absolute errors of PM3 (0.39) and B3LYP/3-21G (0.35) being larger than those of the other methods (0.18~0.22), which indicates that the 6-31G, 6-31G*, 6-31G**, 6-311G*, and 6-31+G** basis sets are more suitable for nitrates. Figure 3 presents the error analysis of the densities calculated with the B3LYP functional and these five basis sets. It is obvious that the errors for PETN (24) and Me-NENA (27) are extraordinarily small (< 0.1) while those of the other 29 aliphatic nitrates are larger than 0.1.

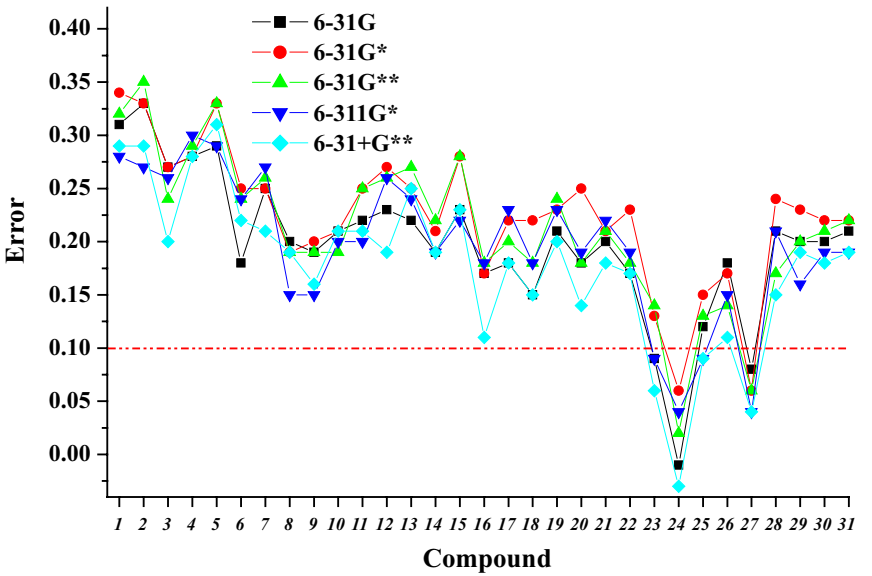

Figure 3. Error analysis of the densities calculated with the B3LYP functional and various basis sets

Table 3 displays the relationships and the corresponding correlation coefficients (R) between the predicted densities with these five basis sets and the experimental densities. For all 31 compounds (set I), the correlation coefficients were 0.9425, 0.9469, 0.9357, 0.9417 and 0.9330, respectively. When the two compounds (24 and 27), which have abnormally small calculation errors, were excluded (set II), the Rs were improved to 0.9641, 0.9682, 0.9584, 0.9601 and 0.9565, respectively. This suggests that these five basis sets can be used to accurately predict the crystalline densities of aliphatic nitrates using the fitting equations.

Table 3. Correlations between the predicted and experimental densities[a]

Method	Set I (1-31)[b]	Set II (1-23, 25, 26, 28-31)[b]
B3LYP/6-31G	$\rho_{cal} = 0.5356 + 0.7634\rho_{exp}$ R = 0.9425 SD = 0.0517	$\rho_{cal} = 0.4567 + 0.8247\rho_{exp}$ R= 0.9641 SD = 0.0420
B3LYP/6-31G*	$\rho_{cal} = 0.5419 + 0.7767\rho_{exp}$ R = 0.9469 SD = 0.0504	$\rho_{cal} = 0.4768 + 0.8283\rho_{exp}$ R = 0.9682 SD = 0.0396
B3LYP/6-31G**	$\rho_{cal} = 0.5724 + 0.7467\rho_{exp}$ R = 0.9357 SD = 0.0538	$\rho_{cal} = 0.5006 + 0.8031\rho_{exp}$ R = 0.9584 SD = 0.0442
B3LYP/6-311G*	$\rho_{cal} = 0.5070 + 0.7826\rho_{exp}$ R = 0.9417 SD = 0.0534	$\rho_{cal} = 0.4451 + 0.8317\rho_{exp}$ R = 0.9601 SD = 0.0448
B3LYP/6-31+G**	$\rho_{cal} = 0.5754 + 0.7220\rho_{exp}$ R = 0.9330 SD = 0.0532	$\rho_{cal} = 0.5011 + 0.7801\rho_{exp}$ R = 0.9565 SD = 0.0440

[a] *R* and SD denote the correlation coefficient and standard deviation, respectively
[b] 1-31 present the serial numbers of the compounds listed in Table 2

According to our results, B3LYP/6-31G* gives the best results, with B3LYP/6-31G leading to the next best results; they require comparatively less computer resources than other methods, therefore, using B3LYP/6-31G* or B3LYP/6-31G is a good choice to rapidly and accurately predict the crystalline densities of aliphatic nitrates. Taking B3LYP/6-31G and B3LYP/6-31G* as examples, Figure 4 shows good correlations between the experimental and theoretical densities for 29 listed compounds (1-23, 25, 26, 28-31). The correlation equations are:

$$\rho_{cal} = 0.4567 + 0.8247\rho_{exp} \quad (4)$$

$$\rho_{cal} = 0.4768 + 0.8283\rho_{exp} \quad (5)$$

$$\rho_{exp} = -0.4153 + 1.1271\rho_{cal} \quad (6)$$

$$\rho_{exp} = -0.4514 + 1.1318\rho_{cal} \quad (7)$$

Equations 6 and 7 can be used to estimate the experimental density from the theoretical density calculated at the B3LYP/6-31G and B3LYP/6-31G* levels, respectively.

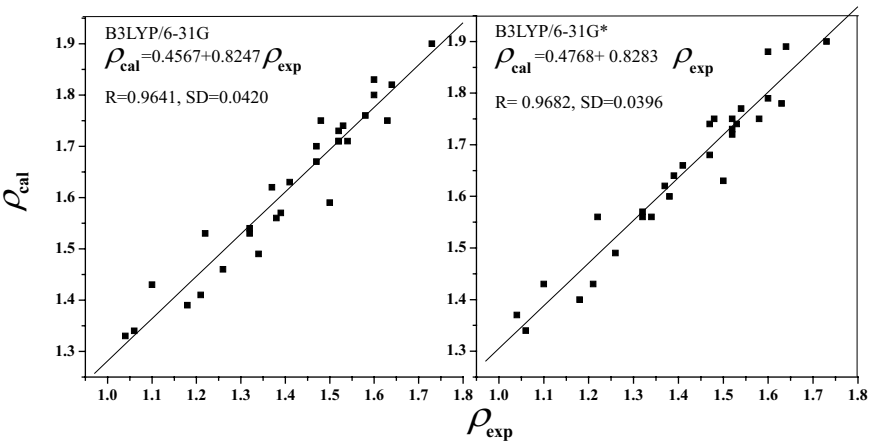

Figure 4. Correlations between the experimental and theoretical densities of the 29 compounds (1-23, 25, 26, 28-31) at the B3LYP/6-31G and B3LYP/6-31G* levels

Table 4 lists the predicted crystalline densities of the 31 nitrates using these equations. To test the reliability of our method, the methods developed by Keshavarz [17] and Politzer [22] have also been adopted to predict the crystal densities of the same nitrates. The densities (ρ_K) estimated with the Keshavarz's method [17] using Equation 8 are also listed in Table 4. Since the densities of the title compounds in this paper were calculated using the B3LYP functional with the different basis sets, *viz*. 6-31G* and 6-31G**, the densities (ρ_R) predicted by Rice [24] with Equation 9 are also presented in Table 4.

$$\rho_K = 1.521 + 6.946a/M - 11.53b/M + 20.10c/M - 0.1559E_D + 0.1325E_I \quad (8)$$

$$\rho_R = 1.0462\rho_{cal} + 0.0021v\sigma_{tot}^2 - 0.1586 \quad (9)$$

where a, b and c in Equation 8 are the numbers of carbon, hydrogen and nitrogen atoms, respectively; the values of E_D and E_I, which are specified based on the molecular structures, were taken from Ref. [17]. ρ_{cal} in Equation 9 is equal to M/V, with V being produced at the B3LYP/6-31G** level (see Table 1).

It can be seen from Table 4 that the average absolute errors (0.04) and root mean square errors (0.05) of the densities predicted with Equations 6 and 7 are significantly reduced in comparision with those in Table 2.

Table 4. A comparison of the densities obtained with our method (ρ'_{exp}), Keshavarz's method (ρ_K) and Rice's results (ρ_R)

Compd. (see Table 1)	ρ_{exp}	6-31G		6-31G*		Keshavarz's method		Rice's results[d]			
	[g·cm^{-3}]	ρ'_{exp} [g·cm^{-3}]	D^a [g·cm^{-3}]	ρ'_{exp} [g·cm^{-3}]	D^a [g·cm^{-3}]	ρ_K [g·cm^{-3}]	$D_K{}^b$ [g·cm^{-3}]	ρ_R [g·cm^{-3}]	$D_R{}^c$ [g·cm^{-3}]	v	$\sigma_{tot}{}^2$ [(kcal·mol^{-1})^2]
1	1.22	1.31	0.09	1.31	0.09	1.158	0.06	1.49	0.27	0.2499	76.76
2	1.10	1.20	0.10	1.17	0.07	1.105	–0.00	1.39	0.29	0.2354	69.15
3	1.48	1.56	0.08	1.53	0.05	1.457	0.02	1.67	0.19	0.1818	88.92
4	1.06	1.10	0.04	1.07	0.01	1.065	–0.00	1.29	0.23	0.2350	71.26
5	1.04	1.08	0.04	1.10	0.06	1.065	–0.02	1.30	0.26	0.1993	67.98
6	1.39	1.35	–0.04	1.40	0.01	1.355	0.03	1.60	0.21	0.2333	111.84
7	1.37	1.41	0.04	1.38	0.01	1.355	0.01	1.59	0.22	0.2100	102.12
8	1.60	1.61	0.01	1.57	–0.03	1.624	–0.02	1.75	0.15	0.1223	124.27
9	1.52	1.51	–0.01	1.50	–0.02	1.529	–0.01	1.69	0.17	0.1945	147.13
10	1.53	1.55	0.02	1.52	–0.01	1.538	–0.01	1.64	0.11	0.0009	83.36
11	1.41	1.42	0.01	1.43	0.02	1.444	–0.03	1.66	0.25	0.2483	153.32
12	1.47	1.50	0.03	1.52	0.05	1.515	–0.05	1.70	0.23	0.1761	135.42
13	1.32	1.32	0.00	1.33	0.01	1.386	–0.07	1.54	0.22	0.2434	73.40
14	1.52	1.51	–0.01	1.51	–0.01	1.552	–0.03	1.71	0.19	0.1566	144.51
15	1.60	1.65	0.05	1.68	0.08	1.650	–0.05	1.84	0.24	0.0997	160.77
16	1.73	1.73	0.00	1.70	–0.03	1.676	0.05	1.87	0.14	0.0984	138.50
17	1.38	1.34	–0.04	1.36	–0.02	1.397	–0.02	1.54	0.16	0.2460	92.04
18	1.34	1.26	–0.08	1.31	–0.03	1.286	0.05	1.47	0.13	0.2497	80.12
19	1.52	1.53	0.01	1.53	0.01	1.541	–0.02	1.73	0.21	0.1840	128.47
20	1.64	1.64	0.00	1.69	0.05	1.657	–0.02	1.80	0.16	0.1233	206.95
21	1.47	1.47	0.00	1.45	–0.02	1.487	–0.02	1.63	0.16	0.1918	88.79
22	1.54	1.51	–0.03	1.55	0.01	1.542	–0.00	1.71	0.17	0.1657	206.26
23	1.50	1.38	–0.12	1.39	–0.11	1.429	0.07	1.59	0.09	0.1920	80.79

24	1.77	–	–	–	–	1.726	0.04	1.78	0.01	0.1677	191.73
25	1.63	1.56	–0.07	1.56	–0.07	1.532	0.10	1.77	0.14	0.1949	208.26
26	1.58	1.57	–0.01	1.53	–0.05	1.505	0.08	1.72	0.14	0.1769	215.83
27	1.53	–	–	–	–	1.232	0.30	1.58	0.05	0.2495	152.75
28	1.32	1.31	–0.01	1.31	–0.01	1.433	–0.11	1.49	0.17	0.2500	164.66
29	1.26	1.23	–0.03	1.23	–0.03	1.356	–0.10	1.45	0.19	0.2500	156.71
30	1.21	1.17	–0.04	1.17	–0.04	1.290	–0.08	1.41	0.20	0.2500	158.84
31	1.18	1.15	–0.03	1.13	–0.05	1.232	–0.05	1.39	0.21	0.2495	152.75
Average absolute error, *Daa*			0.04	–	0.04	–	0.05	–	0.18	–	–
Root mean square error, *Drms*			0.05	–	0.05	–	0.07	–	0.19	–	–

[a] $D = \boldsymbol{\rho}'_{exp} - \boldsymbol{\rho}_{exp}$; [b] $D_K = \rho_K - \boldsymbol{\rho}_{exp}$; [c] $D_R = \rho_R - \boldsymbol{\rho}_{exp;}$ [d] ν and σ_{tot}^2 are calculated using a self-compiled program [52]

Compared with the results from Keshavarz's method (0.05, 0.07) and Rice's method (0.18, 0.19), the present method is slightly better, which indicates that it is reliable and credible to predict $\boldsymbol{\rho}_{exp}$ using the fitting equations at the B3LYP/6-31G and B3LYP/6-31G* levels.

3.2 Effect of molecular structure or substituent groups on density

Data in Table 4 show that the variation in the densities at the B3LYP/6-31G and B3LYP/6-31G* levels is basically consistent. Here, we discuss the effect of structure using the B3LYP/6-31G* results. On the whole, $\boldsymbol{\rho}'_{exp}$, obtained using Equations 6 and 7, increases with an increasing number of $-ONO_2$ groups in the molecule, such as EN (1.17 g·cm^{-3}) and EGDN (1.53 g·cm^{-3}); *n*-PN (1.07 g·cm^{-3}), *iso*-PN (1.10 g·cm^{-3}), 1,3-PGDN (1.40 g·cm^{-3}), 1,2-PGDN (1.38 g·cm^{-3}), and NG (1.57 g·cm^{-3}); 1,2-BGDN (1.33 g·cm^{-3}), 1,2,4-BTTN (1.51 g·cm^{-3}), and ETetN (1.68 g·cm^{-3}). This also indicates that the differences between the $\boldsymbol{\rho}'_{exp}$s of the isomeric compounds, *e.g. n*-PN and *iso*-PN, and 1,3-PGDN and 1,2-PGDN, is very small.

In addition, $\boldsymbol{\rho}'_{exp}$ also increases with an increasing number of –OH, –Cl and –O– groups. For example, $\boldsymbol{\rho}'_{exp}$s of 1,3-PGDN (6) and GDN (9), 1,2-PGDN (7) and GCDN (10) are 1.40 and 1.50 g·cm^{-3}, 1.38 and 1.52 g·cm^{-3}, respectively. However, when more $-CH_2-$ groups are introduced, $\boldsymbol{\rho}'_{exp}$ decreases. This can be found with MN (1.31 g·cm^{-3}) and EN (1.17 g·cm^{-3}), and also with Me-NENA (27), Et-NENA (28), Pr-NENA (29), Bu-NENA (30), and Pt-NENA (31), for which the ρ_{cal} values are 1.59, 1.56, 1.49, 1.43, and 1.40 g·cm^{-3}, respectively, and the $\boldsymbol{\rho}_{exp}$ values are 1.53, 1.32, 1.26, 1.21, and 1.18 g·cm^{-3}, respectively. With the increase in the number of $-CH_2-$ groups from compound (27) to compound (31), the density decreases consecutively by 0.03, 0.07, 0.06, and 0.03 g·cm^{-3} according to ρ_{cal}, and 0.21, 0.06, 0.05, and 0.03 g·cm^{-3} according to $\boldsymbol{\rho}_{exp}$. Obviously, $\boldsymbol{\rho}_{exp}$ of (27) is abnormal. Similarly, for compounds (20) and (24), with the increase in the number of the $-CH_2-$ groups, ρ_{cal} decreases (1.89 and 1.83 g·cm^{-3}, respectively), but $\boldsymbol{\rho}_{exp}$ increases (1.64 and 1.77 g·cm^{-3}), so $\boldsymbol{\rho}_{exp}$ of (24) is possibly abnormal too. Therefore, compounds (24) and (27) are excluded in set II to fit the correlating equation, and the correlation coefficient and deviation are obviously increased and reduced respectively after (24) and (27) are excluded, in comparison with set I where all compounds are included.

In other words, the number of the $-ONO_2$ group has the biggest influence on the density of aliphatic nitrates, and the influence of other groups is also non-negligible. The regularity of the effect of various groups on the density can therefore be applied in the molecular design of energetic materials.

4 Conclusions

From this study, the following conclusions are drawn:

(1) The densities of aliphatic nitrates calculated by various methods are all overestimated in comparision with the experimental densities; the methods in combination the B3LYP functional with the 6-31G, 6-31G*, 6-31G**, 6-311G*, and 6-31+G** basis sets are comparatively better when the fitting equations are used.

(2) Considering the results of and the resources required for these calculations, the B3LYP/6-31G* or B3LYP/6-31G method is recommended for predicting the crystal densities using the fitting equations.

(3) Densities of the aliphatic nitrates increase with an increasing number of $–ONO_2$, –OH, –Cl, and –O– groups, while they decrease with the number of $–CH_2–$ groups, the $–ONO_2$ group having the largest influence on the density.

Acknowledgements

We gratefully thank the National Natural Science Foundation of China (no. 21403110) for its support for this work.

References

[1] Gilbert, P.S.; Jack, A. Research Towards Novel Energetic Materials. *J. Energetic Mater.* **1986**, *45*: 5-28.

[2] Agrawal, P.J. Recent Trends in High-energy Materials. *Prog. Energy Combust. Sci.* **1998**, *24*: 1-30.

[3] Zhang, M.X.; Eaton, P.E.; Gilardi, R. Hepta- and Octa-nitrocubane. *Angew. Chem. Int. Ed.* **2000**, *39*: 401-404.

[4] Kamlet, M.J.; Jacobs, S.J. Chemistry of Detonations. I. A Simple Method for Calculating Detonation Properties of C-H-N-O Explosives. *J. Chem. Phys.* **1968**, *48*: 23-35.

[5] Zhang, X.H.; Yun, Z.H. *Explosive Chemistry*. National Defence Industry Press, Beijing, People's Republic of China, **1989**, ISBN: 9787118076479.

[6] Tarver, C.M. Density Estimations for Explosives and Related Compounds Using the Group Additivity Approach. *J. Chem. Eng. Data* **1979**, *24*:136–145.

[7] Stine, J.R. *Prediction of Crystal Densities of Organic Explosives by Group Additivity*. Los Alamos National Laboratory's Report, New Mexico, **1981**.

[8] Ammon, H.L. New Atom/Functional Group Volume Additivity Data Bases for the Calculation of the Crystal Densities of C-, H-, N-, O-, F-, S-, P-, Cl-, and Br-containing Compounds. *Struct. Chem.* **2001**, *12*: 205-212.

[9] Karfunkel, H.R.; Gdanitz, R.J. *Ab Initio* Prediction of Possible Crystal Structures for General Organic Molecules. *J. Comp. Chem.* **1992**, *13*: 1171-1183.
[10] Holden, J.R.; Du, Z.; Ammon, H.L. Prediction of Possible Crystal Structures for C, H, N, O, and F Containing Organic Compounds. *J. Comp. Chem.* **1993**, *14*: 422-437.
[11] Pivina, T.S.; Shcherbukhin, V.V.; Molchanova, M.S.; Zefirov, N.S. Computer-assisted Prediction of Novel Target High-energy Compounds. *Propellants Explos. Pyrotech.* **1995**, *20*: 144-146.
[12] Dzyabchenko, A.V.; Pivina, T.S.; Arnautova, E.A. Prediction of Structure and Density for Organic Nitramines. *J. Mol. Struct*. **1996**, *378*: 67-82.
[13] Rice, B.M.; Sorescu, D.C. Assessing a Generalized CHNO Intermolecular Potential Through *Ab Initio* Crystal Structure Prediction. *J. Phys. Chem. B* **2004**, *108*: 17730-17739.
[14] Keshavarz, M.H. New Method for Calculating Densities of Nitroaromatic Explosive Compounds. *J. Hazard. Mater.* **2007**, *45*: 263-269.
[15] Keshavarz, M.H. Prediction of Densities of Acyclic and Cyclic Nitramines, Nitrate Esters and Nitroaliphatic Compounds for Evaluation of Their Detonation Performance. *J. Hazard. Mater.* **2007**, *143*: 437-442.
[16] Keshavarz, M.H. Novel Method for Predicting Densities of Polynitro Arene and Polynitro Heteroarene Explosives in Order to Evaluate Their Detonation Performance. *J. Hazard. Mater.* **2009**, *165*: 579-588.
[17] Keshavarz, M.H.; Pouretedal, H.R. A Reliable Simple Method to Estimate Density of Nitroaliphatics, Nitrate Esters and Nitramines. *J. Hazard. Mater.* **2009**, *169*: 1581-69.
[18] Keshavarz, M.H.; Motamedoshariati, H.; Moghayadnia, R.; Ghanbarzadeh, M.; Azarniamehraban, J. A New Computer Code for Assessment of Energetic Materials with Crystal Density, Condensed Phase Enthalpy of Formation, and Activation Energy of Thermolysis. *Propellants Explos. Pyrotech.* **2013**, *38*: 95-102.
[19] Keshavarz, M.H.; Soury, H.; Motamedoshariati, H.; Dashtizadeh, A. Improved Method for Prediction of Density of Energetic Compounds Using Their Molecular Structure. *Struct. Chem.* **2015**, *26*:455-466.
[20] Keshavarz, M.H.; Rahimi, R.; Akbarzadeh, A.R. Two Novel Correlations for Assessment of Crystal Density of Hazardous Ionic Molecular Energetic Materials Using Their Molecular Structures. *Fluid Phase Equilib.* **2015**, *402*:1-8.
[21] Rahimi, R.; Keshavarz, M.H.; Akbarzadeh, A.R. Prediction of the Density of Energetic Materials on the Basis of their Molecular Structures. *Cent. Eur. J. Energ. Mater.* **2016**, *13*: 73-101.
[22] Politzer, P.; Martinez, J.; Murray, J.S.; Concha, M.C.; Toro-Labbé, A. An Electrostatic Interaction Correction for Improved Crystal Density Prediction. *Mol. Phys*. **2009**, *107*: 2095-2101.
[23] Politzer, P.; Martinez, J.; Murray, J.S.; Concha, M.C. An Electrostatic Correction for Improved Crystal Density Predictions of Energetic Ionic Compounds. *Mol. Phys.* **2010**, *108*: 1391-1396.
[24] Rice, B.M.; Byrd, E.F.C. Evaluation of Electrostatic Descriptors for Predicting Crystalline Density. *J. Comput. Chem.* **2013**, *34*: 2146-2151.

[25] Zhang, J.; Xiao, H.M. Computational Studies on the Infrared Vibrational Spectra, Thermodynamic Properties, Detonation Properties and Pyrolysis Mechanism of Octanitrocubane. *J. Chem. Phys.* **2002**, *116*: 10674-10683.
[26] Xu, X.J.; Xiao, H.M.; Gong, X.D.; Ju, X.H.; Chen, Z.X. Theoretical Studies on the Vibrational Spectra, Thermodynamic Properties, Detonation Properties and Pyrolysis Mechanisms for Polynitroadamantanes. *J. Phys. Chem. A* **2005**, *109*: 11268-11274.
[27] Xu, X.J.; Xiao, H.M.; Ju, X.H.; Gong, X.D.; Zhu, W.H. Computational Studies on Polynitro- Hexaazaadmantanes as Potential High Energy Density Materials (HEDMs). *J. Phys. Chem. A* **2006**, *110*: 5929-5933.
[28] Qiu, L.; Xiao, H.M.; Gong, X.D.; Ju, X.H.; Zhu, W.H. Theoretical Studies on the Structures, Thermodynamic Properties, Detonation Properties, and Pyrolysis Mechanisms of Spiro Nitramines. *J. Phys. Chem. A* **2006**, *110*: 3797-3807.
[29] Xiao, H.M.; Xu, X.J.; Qiu, L. *Theoretical Design of High Energy Density Materials*. Science Press, Beijing, **2008**; ISBN 9787030206190.
[30] Wang, G.X.; Shi, C.H.; Gong, X.D.; Xiao, H.M. Theoretical Investigation on Structures, Density, Detonation Properties and Pyrolysis Mechanism of the Derivatives of HNS. *J. Phys. Chem. A* **2009**, *113*: 1318-1326.
[31] Qiu, L.M.; Gong, X.D.; Wang, G.X.; Zheng, J.; Xiao, H.M. Looking for High Energy Density Compounds among 1,3-Bishomopentaprismane Derivatives with –CN, –NC, and $–ONO_2$ Group. *J. Phys. Chem. A* **2009**, *113*: 2607-2614.
[32] Qiu, L.; Xiao, H.M.; Gong, X.D. Ju, X.H.; Zhu, W. Crystal Density Predictions for Nitramines Based on Quantum Chemistry. *J. Hazard. Mater.* **2007**, *141*: 280-288.
[33] Wang, G.X.; Gong, X.D.; Liu, Y.; Du, H.C.; Xiao, H.M. Prediction of Crystalline Densities of Polynitro Arenes for Estimation of Their Detonation Performance Based on Quantum Chemistry. *THEOCHEM* **2010**, *953*(1): 163-169.
[34] Brand, J.C.D.; Cawthon, T.M. The Vibrational Spectrum of Methyl Nitrate. *J. Am. Chem. Soc.* **1955**, *77*: 319-323.
[35] Gong, X.D.; Xiao, H.M. *Ab Initio* and Density Functional Methods Studies on the Conformations and Thermodynamic Properties of Propyl Nitrate. *THEOCHEM* **2000**, *498*: 181-190.
[36] Türker, L.; Erkoç, Ş. Density Functional Theory Calculations for $[C_2H_4N_2O_6]^{(n)}$ ($n = 0, +1, -1$). *J. Hazard. Mater. A* **2006**, *136*: 164-169.
[37] Li, M.M.; Wang, G. X.; Guo, X.D.; Song, H.C. Theoretical Study on the Vibrational Spectra, Thermodynamic Properties, Density, Detonation Properties and Pyrolysis Mechanism of Four Trinitrate Esters. *THEOCHEM* **2009**, *100:* 90-95.
[38] Stewart, J.J.P. Optimization of Parameters for Semiempirical Methods. I. Method. *J. Comput. Chem*. **1989**, *10*: 209-220.
[39] Lee, C.; Yang, W.; Parr, R.G. Development of the Colle-Salvetti Correlation-energy Formula into a Functional of the Electron Density. *Phys. Rev. B* **1988**, *37*: 785-789.
[40] Becke, A.D. Density-functional Thermochemistry, II. The Effect of the Perdew-Wang Generalized-gradient Correlation Correction. *J. Chem. Phys.* **1992**, *97*: 9173-9177.

[41] Binkley, J.S.; Pople, J.A.; Hehre, W.J. Self-consistent Molecular Orbital Methods. 21. Small Split-valence Basis Sets for First-row Elements. *J. Am. Chem. Soc.* **1980**, *102*: 939-947.
[42] Rassolov, V.A.; Ratner, M.A.; Pople, J.A .; Redfern, P.C.; Curtiss, L.A. 6-31G* Basis Set for Third-row Atoms. *J. Comp. Chem.* **2001**, *22*: 976-984.
[43] Hariharan, P.C.; Pople, J.A. Influence of Polarization Functions on MO Hydrogenation Energies. *Theor. Chim. Acta* **1973**, *28*: 213-222.
[44] Petersson, G.A.; Al-Laham, M.A. A Complete Basis Set Model Chemistry. II. Open-shell Systems and the Total Energies of the First-row Atoms. *J. Chem. Phys.* **1991**, *94*: 6081-6090
[45] McLean, A.D.; Chandler, G.S. Contracted Gaussian Basis Sets for Molecular Calculations, I. Second Row Atoms, Z = 11-18. *J. Chem. Phys*. **1980**, *72*: 5639-5648.
[46] Frisch, M.J.; Trucks, G.W.; Schlegel, H.B.; Scuseria, G.E.; Robb, M.A.; Cheeseman, J.R.; Montgomery, J.A.; Vreven, J.T.; Kudin, K.N.; Burant, J.C,; Millam, J.M.; Iyengar, S.S.; Tomasi, J.; Barone, V.; Mennucci, B.; Cossi, M.; Scalmani, G.; Rega, N.; Petersson, G.A.; Nakatsuji, H.; Hada, M.; Ehara, M.; Toyota, K.; Fukuda, R.; Hasegawa, J.; Ishida, M.; Nakajima, T.; Honda, Y.; Kitao, O.; Nakai, H.; Klene, M.; Li, X.; Knox, J.E.; Hratchian, H.P.; Cross, J.B.; Adamo, C.; Jaramillo, J.; Gomperts, R.; Stratmann, R.E.; Yazyev, O.; Austin, A.J.; Cammi, R.; Pomelli, C.; Ochterski, J.W.; Ayala, P.Y.; Morokuma, K.; Voth, G.A.; Salvador, P.; Dannenberg, J.J.; Zakrzewski, V.G.; Dapprich, S.; Daniels, A.D.; Strain, M.C.; Farkas, O.; Malick, D.K.; Rabuck, A.D.; Raghavachari, K.; Foresman, J.B.; Ortiz, J.V.; Cui, Q.; Baboul, A.G.; Clifford, S.; Cioslowski, J.; Stefanov, B.B.; Liu, G.; Liashenko, A.; Piskorz, P.; Komaromi, I.; Martin, R.L.; Fox, D.J.; Keith, T.; Al-Laham, M.A.; Peng, C.Y.; Nanayakkara, A.; Challacombe, M.; Gill, P.M.W.; Johnson, B.; Chen, W.; Wong, M.W.; Gonzalez, C.; Pople, J.A. *Gaussian 03*. Gaussian, Inc., Pittsburgh PA, **2003**; ISBN O-9636769-6-2.
[47] Tarver, C.M. Density Estimations for Explosives and Related Compounds Using the Group Additivity Approach. *J. Chem. Eng. Data*. **1979**, *24*: 136-145.
[48] Zhang, X.F. *Performance Manual of Raw and Processed Materials of Overseas Explosives*. Weapon Industry Press, Beijing, **1991**; ISBN 9787801726353.
[49] Zhong, Y.P.; Hu, Y.D.; Jiang, H.Z. *Performance Manual of Overseas Explosives*. Weapon Industry Press, Beijing, **1990**; ISBN 9787802485990.
[50] Dong, H.S.; Zhou, F.F. *High Energy Explosives and Their Corresponding Performance*. Science Press, Beijing, **1989**; ISBN 9787030206190.
[51] Chen, Z.H. *Explosives Manual*. China Coal Industry Publishing House, **1980**; ISBN 7502001085.
[52] Gong, X.D. Potden v.2.0. Nanjing. Nanjing University of Science and Technology, **2007**.

Received: September 7, 2018
Revised: September 12, 2019
First published online: September 20, 2019